

α -Particle Interactions in Nuclear Emulsion for Hadron Therapy and shielding Elaboration

H. A. Amer, M. M. El-Ashmawy and N. Abdallah

Nuclear and Radiological Regulatory Authority, ENRRA, Egypt.

Abstract: 2.1A and 3.7A GeV α -Particles from Dubna Synchrophasetron are used to understand and address some effects in hadron therapy and shielding programming. The NIKFI-BR2 nuclear emulsion is the present target nuclei, like-some human and shield materials. The interaction mean free path with HCNO nuclei is determined. The inelastic interaction cross section is approximated by a power law, which is independent on the energy and expressed in terms of the target mass number. The different characteristics of the present projectile and target fragmentations are investigated experimentally in comparison with the SRIM simulations

Keywords: Nuclear Emulsion / High-Energy α -Particles / Some Simulations for Hadron Therapy and Shielding Programs.

I. Introduction

At low energy the physics can be accounted for fairly well by one single source. The de-excitation can be understood in terms of particle emission from a liquid drop of nuclear matter. At high energy, multiple sources are needed. The de-excitation is here understood in terms of particle emission from an expanding gas of nuclear matter in thermodynamical equilibrium. At excitation energies comparable with the total binding energy, $\sim 5A$ to $8A$ MeV, the very existence of a long-lived compound nucleus becomes unlikely. In this situation an explosion-like process leads to the total disintegration of the nucleus and the multiple emission of nuclear fragments of different masses (1 and references therein). One can come to the multifragmentation concept from a quite different starting point, by considering a liquid-gas phase transition in excited nuclear matter. The name "multifragmentation" is introduced firstly in Ref. (2). At high energy collisions, the produced particles are not confined up to nuclear fragments but they include essentially created particles the so called hadrons.

It is known that, the radiation therapy is the medical use of ionizing radiation to treat cancer. In conventional radiation therapy, beams of X-rays (high energy photons) are produced by accelerated electrons and then delivered to the patient to destroy tumor cells. Using crossing beams from many angles, radiation oncologists irradiate the tumor target while trying to spare the surrounding normal tissues. Inevitably some radiation dose is always deposited in the healthy tissues. Initially, the clinical applications are limited to few parts of the body since the accelerators are not powerful enough to allow protons to penetrate deep in the tissues. The improvements in accelerator technology coupled with advances in medical imaging and computing, make proton therapy a viable option for routine medical applications. Therefore, proton becomes the most common type of particle therapy. However, the photon as a particle is used in X-ray and γ -ray, the so called photon therapy. Muon and electron, the so called lepton therapy, are occasionally attempted. All the particles that are constructed of quarks (hadrons) are not elementary. Therefore, in their usage, it is more correctly to say hadron therapy. When the irradiating beams are made of charged particles (protons, α -particle, and heavier ions), radiation therapy is also called hadron therapy or heavy-ion therapy. The strength of hadron therapy lies in the unique physical and radiobiological properties of these particles. They can penetrate the tissues with little diffusion and deposit the maximum energy just before stopping. This allows a precise definition of the specific region to be irradiated. With the use of the hadron the tumor can be irradiated while the damage to healthy tissues is less than with X-rays. Although protons are used in several hospitals, the next step in radiation therapy is the use of carbon ions. These have some clear advantages even over protons in providing both a local control of very aggressive tumors and a lower acute or late toxicity. At HIMAC (NIRS, Chiba, Japan) Kanai et al Ref. (3 and references therein) study the fragmentation of (0.09A and 0.5A GeV iron) and 0.4A GeV krypton beams in tissue equivalent material. For radiotherapy at GSI (Darmstadt, Germany) information on carbon fragmentation in tissue-like materials is of great interest^(4, 5). For shielding applications, relatively light ions such as helium, carbon, neon, and silicon are worth studying both in their own right and because they are produced as secondary fragments by interactions of heavier primary ions in shielding and in the human body. In support of the HIMAC radiotherapy program, Kanai et al Ref. (3 and references therein) use the fragmentation of (0.15A GeV, 0.29A, and 0.4A GeV) ^{12}C , 0.4A GeV ^{20}Ne , 0.49A GeV ^{28}Si , and 0.55A GeV ^{40}Ar on $\text{C}_3\text{H}_8\text{O}_2$ target. Malakhov et al Ref. (3 and references therein) measure fragments produced by a 1.044A GeV d beam in a gold target at the Nuclotron of Dubna, Russia. Although these measurements are with a heavy target, the

number of light ions produced in secondary collisions makes them relevant, and argues for further measurements, perhaps with shielding and tissue equivalent targets. At Lawrence Berkeley National Laboratory, LBNL, of USA Miller present measurements for hadron therapy over energy range of 0.1A up to 1A GeV[3]. At the end of 2008, about 28 treatment facilities are in operation worldwide and over 70,000 patients can be treated by means of pions[6–8], protons, and heavier ions. In Europe, the interest in hadron therapy grows rapidly and the first heavy-ion clinical facility in Heidelberg, Germany, starts treating patients at the end of 2009[9]. While the advantages of protons over photons are quantitative in terms of the amount and distribution of the delivered dose, several studies show evidence that carbon ions damage cancer cells in a way that the cells can not repair themselves. Carbon therapy may be the optimal choice to tackle radio-resistant tumors; other light ions, such as helium, are also being investigated[10].

On the other hand, the high-energy hadron-hadron, hadron-nucleus, or nucleus-nucleus interactions are a precise source in which all categories of secondary emitted particles are available. It is very important to learn as much as possible about all the phenomena which occur in this interactions to observe the anticipated signatures on the background of "normal phenomena". Some of these phenomena are the hadron production, projectile fragmentation, target fragmentation, the multiplicity and emission characteristics, the reaction cross sectional behavior, and the stopping power of the target materials in the voted detector with respect to each passing particle. Hence, the choice of projectiles, targets, energies, and the critical parameters in measurements motivates the correct modeling and simulation of the therapy planning. Actually, the synchrotron accelerator at Dubna enables equipping beams of $A_{\text{Proj}} \geq 1$, in a few A GeV ranges of energies. This region is a special energy, at which the nuclear limiting fragmentation applies initially[11–17]. The nuclear emulsion is a very useful tool in experimental physics for investigating atomic and nuclear processes. It can be used as a detector of 4- π space geometry. It contains target materials over a wide range of mass numbers, ^1H , ^{12}C , ^{14}N , ^{16}O , ^{82}Br , ^{108}Ag . It has the possibility of measuring energies and angles with high degree of resolution. It can be used in studying the characteristics of new elementary particles and can detect the decay of the unstable neutral particles, rather than, its sensitivity to slow charged particles arising from the disintegration of the target nucleus. Owing to the high stopping power of emulsion, a large fraction of short-lived particles is brought to rest in it before decay and hence their ranges and life times can be measured accurately. In this work the interactions of α -particle with emulsion nuclei are studied at Dubna energies (2.1A and 3.7A GeV).

II. Experimental Details

This work is carried out using a nuclear emulsion stack of type NIKFI-BR2 where the dimensions of each pellicle are 10 cm \times 20 cm \times 600 μm . The stacks are exposed to 2.1A and 3.7A GeV ^4He ion beams from JINR Synchrotron at Dubna, Russia. Each stack has a sensitivity of about 30 grains per 100 μm for singly charged minimum ionizing particles. The secondary tracks emerging from each interaction are classified according to the emulsion terminology[18, 19] depending on their appearance under the microscope. These tracks are shower (N_s), grey (N_g), or black (N_b) ones. The shower tracks ($\beta \geq 0.7$) correspond to singly charged relativistic particles (mainly pions with kinetic energy > 70 MeV), while the grey ($0.3 \leq \beta \leq 0.7$) and black ($\beta < 0.3$) tracks are produced by comparatively slower fragments emitted from the target nucleus. The grey tracks are mostly recoil target protons with kinetic energy $26 \leq \text{K.E} \leq 400$ MeV while the black tracks are due to protons of kinetic energy < 26 MeV. The grey and black tracks are denoted as tracks of heavily ionizing particles N_h , i.e. $N_h = N_g + N_b$.

III. Results and Discussions

The nuclear fragmentation complicates both shielding design and treatment planning for the hadron therapy. The required data can be the interaction cross section, fragmentation cross section, and fluence. The interaction cross section is the probability that the projectile nucleus collides with the target nucleus at certain impact parameter and energy. The fragmentation cross section is the probability that the nuclear collision can produce a nuclear fragment. The fluence is the number of fragments produced at depth in shielding material. Hence, it is necessary to study the multiplicity characteristics, angular characteristics, and ionization behavior of the nuclear fragments.

Interaction Characteristics

It is known that the human body is nearly 57% water. Since the water molecule is H_2O , then the hydrogen is about 11% while the oxygen is 67% by the count of atoms. Therefore, the majority of the human body mass is oxygen. The most abundant materials in the human body are O, C, H, and N. Their percentages are nearly 65, 18.5, 9.5, and 3.2%, respectively. Table (1) shows the present emulsion chemical composition.

Table (1): The chemical composition of NIKFI–BR2 emulsion.

Element	¹ H	¹² C	¹⁴ N	¹⁶ O	⁸⁰ Br	¹⁰⁸ Ag
Atoms /cm ³ ×10 ²²	3.150	1.410	0.395	0.956	1.028	1.028

From Table (1) one can show that the most abundant human materials are enclosed in the nuclear emulsion. Therefore the interactions with emulsion nuclei can be used in simulating the hadron therapy and shielding programs.

To evaluate the interaction effects with the most abundant human materials Table (2) is displayed. In Table (2) the measured mean free paths of light nuclei with HCNO nuclei of emulsion at Dubna energies are listed.

Table (2): Data of Beams interactions with HCNO.

Projectile	E _{lab} GeV/A	L m	N Events	λ cm
p	3.7	799.998	807	99.13±3.49
³ He	3.7	332.600	602	55.25±2.25
⁴ He	2.1	416.500	723	57.61±2.14
⁴ He	3.7	217.600	394	55.23±2.78
⁶ Li	3.7	148.450	398	37.30±1.87
⁷ Li	2.2	153.500	402	38.18±1.90

To give a systematic evaluation of these interactions the mean free paths are correlated with A_{Proj} in Fig. (1).

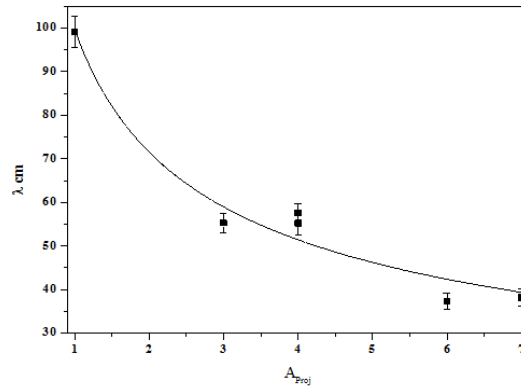


Figure (1): The dependence of the mean free path on the projectile mass numbers at Dubna energies.

The data of Fig. (1) are approximated by the power law relation of Equation (1) which is presented by the smooth curve.

$$\lambda = aA_{Proj}^b \text{ cm(1)}$$

The fit parameters *a* and *b* are 99.50±4.74 and -0.48±0.04, respectively. The present 2.1A and 3.7A GeV ⁴He inelastic interactions cross sections are correlated with the target mass number in Fig. (2). From Fig. (2), the cross sectional values are nearly the same at the two used energies. The Glauber's approach, encoded in Ref.[20], can predict them well. The data are approximated by the power law relation of Equation (2) which is presented by the smooth curves in Fig. (2). The fit parameters, *c* and *d*, are listed in Table (3). The fit parameters are *c* ~ 120 and *d* = 0.56 ~ 2/3. Therefore, Equation (2) can be rewritten as Equation (3).

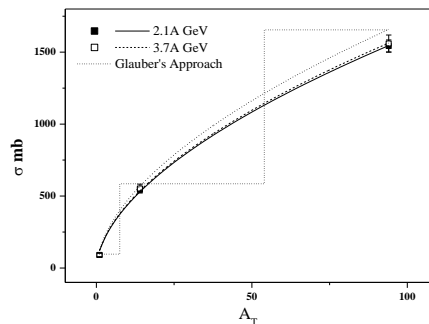


Figure (2): The cross section of the present α-particle inelastic interactions in nuclear emulsion as a function of the target size, together with the predictions of the Glauber's approach (histogram).

$$\sigma = cA_T^d \quad (2)$$

$$\sigma = 120A_T^{0.56} \text{mb} \quad (3)$$

Table (3): The fit parameters of Equation (2).

Fit Parameter	c	d
$E_{\text{lab}} = 2.1\text{A GeV}$	119.74 ± 16.43	0.56 ± 0.03
$E_{\text{lab}} = 3.7\text{A GeV}$	121.46 ± 17.10	0.56 ± 0.03
Glauber's Approach Prediction	128.54 ± 17.88	0.56 ± 0.03

Multiplicity Characteristics

In the high-energy nuclear collisions, the projectile fragments can be distinguished well from the target fragments. In the present interactions the projectile fragments possibilities may be 0, 1, or 2 hydrogen isotopes. They are emitted sharply in the forward narrow cone within $\theta_{\text{lab}} \leq 3^\circ$. The target fragments are nucleons with minor admixture of nuclear isotopes having $Z \leq 2$. They are emitted in the 4π space. For shielding application, relatively light ions such as helium are worth studying both in their own right and because they are produced as secondary fragments by interactions of heavier primary ions in the space craft shielding and in the human body. In Fig. (3) the projectile fragmentation cross section can be approximated, for the present 2.1A and 3.7A GeV ^4He interaction with emulsion nuclei, as a function of Q. Q is the total charge of the projectile fragments. This approximation is presented in Fig. (3) by the smooth curves and determined by the 2nd order polynomial of Equation (4).

$$\sigma = \sum_{i=0}^2 a_i Q_i^i \quad (4)$$

The fit parameters a_0 , a_1 , and a_2 are found (316.80, -61.95, and -28.95) and (238.80, 8.10, and -17.10) according to (2.1A GeV) and (3.7A GeV), respectively.

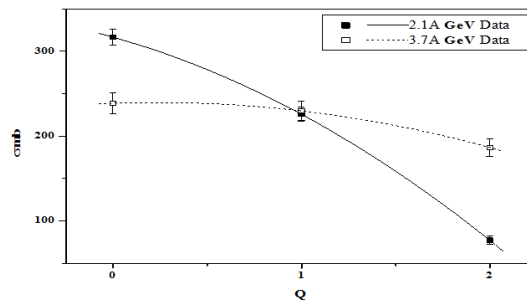


Figure (3): The projectile fragmentation cross section as a function of Q in the present 2.1A and 3.7A GeV ^4He interactions with emulsion nuclei.

Since the majority of the identified target fragments are protons, (> 90%), then their multiplicity, N_h , can amount the target charge. The target fragmentation cross section is displayed in Fig. (4) as a function of N_h for the present 2.1A and 3.7A GeV ^4He interactions with emulsion nuclei. Regarding the nuclear limiting fragmentation in the present energy region the two interactions have no dependence on the energy. As a result of the target composition mixing the distribution shape does not enable to approximate the cross section in a systematic determination law. Hence, it is reasonable to take the target separation methods into consideration.

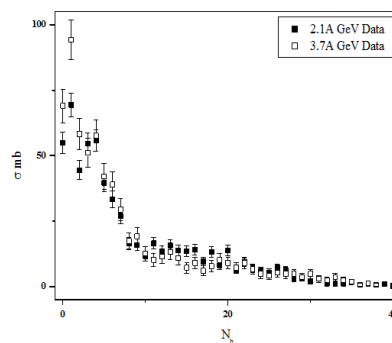


Figure (4): The dependence of the target fragmentation cross section on N_h in the present 2.1A and 3.7A GeV ^4He interactions with emulsion nuclei

Angular Characteristics

The angular distribution of the emitted target protons in the present 3.7A GeV ⁴He interactions with emulsion nuclei is displayed in Fig. (5). This distribution is carried out over a sample of 446 tracks. The laboratory space angles of emission for these tracks are measured using the KSM.1. Carl Zeiss German microscope. This high accurate microscope is widely used to measure the angles and momentum of the tracks as in Ref. [21–23]. From Fig. (5) one observes that the peaking shape is a characteristic of the angular distribution. The distribution is approximated by the Gaussian fit presented in the figure by the smooth dashed curve. The peak of this curve is positioned at $\theta_{lab} \sim 77.95^\circ$. The average emission angle for this sample of tracks $\sim 84.46^\circ$. However the distribution shape tends to have a multimodal nature where three peaks are associated with the angular regions, $0^\circ \leq \theta_{lab} \leq 70^\circ$, $70^\circ \leq \theta_{lab} \leq 120^\circ$, and $120^\circ \geq \theta_{lab}$. In these regions the distributions are fitted by the Gaussian shapes presented by the smooth solid curves. The peaks of these curves are positioned at $\theta_{lab} \sim 58.34^\circ$, 82.77° , and 134.73° according to the three regions, respectively. In the same respect, the average angles of emission are 48.65° , 90.72° , and 140.37° . The average angles of emission are nearly equal to the peak positions. The distribution associated with the region $70^\circ \leq \theta_{lab} \leq 120^\circ$ has nearly the same characteristics as of the total distribution where the peak position and the average angle of emission is $\sim 90^\circ$. Therefore this system can be symmetric in the 4π space with most probable emission at the right angle.

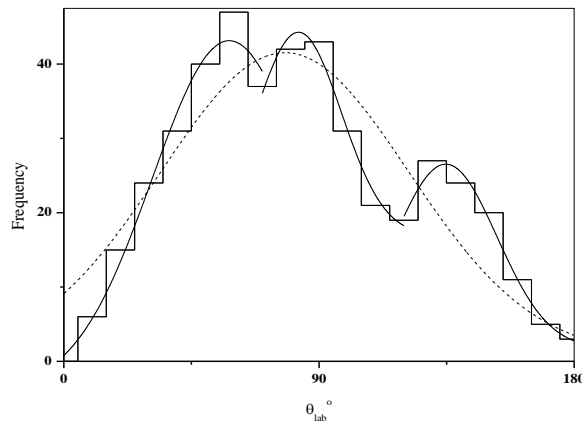


Figure (5): The angular distribution of the emitted target proton in the present 3.7A GeV ⁴He interaction with emulsion nuclei.

Ionization Behavior

The randomly selected tracks from the present 3.7A GeV ⁴He interactions with emulsion nuclei are identified from the relation between $P\beta$ and their relative grain densities. The only tracks identified as target proton fragments are voted. Depending on the kinematical laws, the Coulomb scattering measurements of $P\beta$, the relative grain densities, and the laboratory space angle of emission [18, 19, 24] of each track the energy and range can be determined.

The measured kinetic energy associated with each track of the selected sample ranges nearly from 0 up to 170 MeV. In Fig. (6) the energy range correlation of each measured track is presented. The whole energy range is divided into smaller insets as shown in Fig. (6). In each inset the energy is correlated with energy by a power law relation of Eq. (5). The correlation fitting is presented in Fig. (6) by the smooth curves. The fit parameters g and h are nearly found 0.01 and 1.8, respectively, irrespective of the kinetic energy. Therefore Equation (5) can be rewritten as Equation (6) where the kinetic energy is measured in MeV.

$$R = gE_{lab}^h \quad (5)$$

$$R = 0.01E_{lab}^{1.8} \quad (6)$$

On the basis of the nuclear limiting fragmentation hypothesis the characteristics of the target fragments are limited irrespective of the projectile size or energy. Therefore, Equation (6) is a universal law correlating the kinetic energy with the range of protons through their flight in shields or human body like nuclear emulsion materials. The energy–range relationship of protons in nuclear emulsion is given in text books [25] as, $R = 10.92E_{lab}^{1.72}$, where the range is measured in μm and the kinetic energy in MeV. This agrees with the present results.

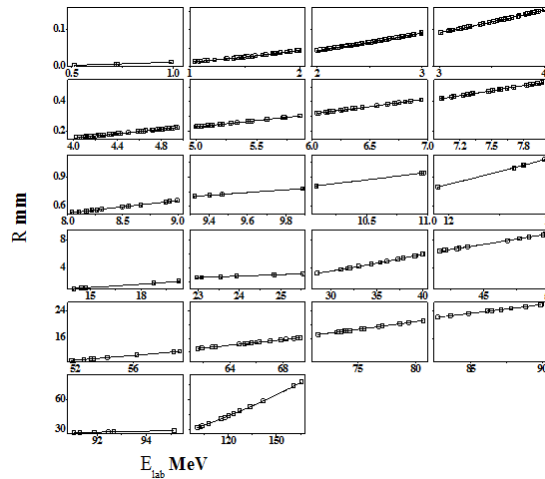


Figure (6): The energy–range correlation for the fragmented target protons in the present 3.7A GeV ⁴He interactions with emulsion nuclei.

In Fig. (7) the SRIM program[26] is used in data simulation. This program is a collection of software packages which can predict the stopping power of different nuclear media and the range traversed by ions. The available range of the incident kinetic energy is 10 KeV up to 4 GeV. In the present work, the SRIM is processed for hydrogen passage in nuclear emulsion at energy range of 1 up to 300 MeV.

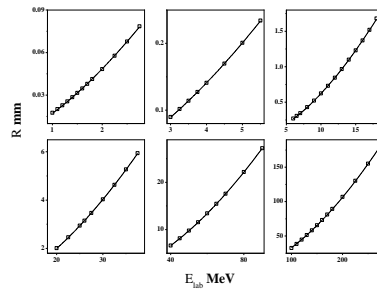


Figure (7): The SRIM simulation of the energy–range correlation for ¹H interacting with emulsion nuclei at energy range up to 300 MeV.

The data can be approximated by Equation (5) where the fitting is presented in Fig. (7) by the smooth curves. The fit parameter *g* is found 0.02, 0.02, 0.01, 0.01, 0.01, and 0.01 according to ascending sort of the energy range in each inset of Fig. (7). In the same respect *h* is found 1.49, 1.59, 1.68, 1.73, 1.74, and 1.68. On average *g* and *h* are 0.01 and 1.7, respectively. This agrees with our experimental results also.

The energy spectrum of the selected sample of the fragmented target protons through the present 3.7A GeV ⁴He interactions with emulsion nuclei is displayed in Fig. (8).

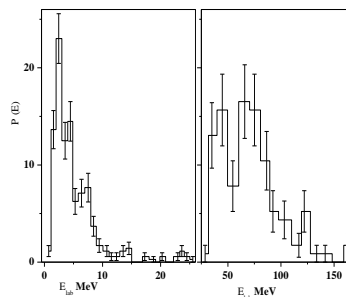


Figure (8): The energy spectrum of the fragmented target protons in the present 3.7A GeV ⁴He interactions with emulsion nuclei.

The two insets of Fig. (8) correspond to average energies ~ 5.21 and 70.67. According to Equation (6) the corresponding ranges are 0.20 and 21.31 mm, respectively.

IV. Conclusions

2.1A and 3.7A GeV α -Particle interactions in nuclear emulsion are efficient for hadron therapy and shielding simulation programs. Actually it is hoped that the models improvement, on the basis of experiment, can reduce the needs of lab equipping and radiation hazard in practice. Accordingly the following conclusions are drawn;

- The nuclearemulson can be used in experiment as target like-human materials where the H, C, N, and O nuclei are enclosed.
- The logarithmicdecrement of α -Particle mean free path in HCNO emulsion nuclei is determined as a function of the target mass number.
- The inelastic interaction cross section of α -Particle with emulsion nuclei is approximated by a universal power law depending on the target mass number only while the energy is not effective. The theoretical simulation of the Glauber's approach results in a successful estimation of the cross section.
- The projectile fragments cross section is approximated by a 2nd order polynomial depending on the total charge of the fragments. The target fragments cross section can not be approximated in a systematic relation with their multiplicity.
- The angular distribution of the target fragments is reproduced well by Gaussian shapes. The most probable emission is located in the region, $70^\circ \leq \theta_{lab} \leq 120^\circ$, with $\langle \theta_{lab} \rangle \sim 90^\circ$.
- The emitted target protons flying in nuclear emulsion have a universal Energy – Range relationship approximated as, $R = 0.01E_{lab}^{1.8}$, where R is measured in mm and E_{lab} in MeV. The SRIM Simulation implies a good agreement.
- The fragmented target protons spectrum is characterized by a peaking shapes both in the region $0 < E_{lab} \leq 26$ MeV, $26 < E_{lab} \leq 160$ MeV.

Finally, more experimental and theoretical activities are efficient in solving more problems of hadron therapy and shielding preparation.

Acknowledgement

The authors express the deeply thanks to Prof. Dr. B.M.Badawy the head of the Reactor Physics Department, Nuclear Research Center, Atomic Energy Authority for great help. Also we thanks very much all members of the emulsion group at M.El-Nadi high energy laboratory in Cairo University We owe much to Vekseler and Baldin High Energy Laboratory, JINR, Dubna, Russia, for supplying us the photographic emulsion plates irradiated at Synchrophasotron.

References

- [1]. J. P. Bondorf, A. S. Botvina, A. S. Iljinov, I. N. Mishustin, and K. Sneppen, Phys. Rep. 257, 133 (1995).
- [2]. J. P. Bondorf; Journal de Physique 37/C5, 195 (1976), Proceeding of the EPS topical conference on Large Amplitude Collective Nuclear Motions, Keszthely, Hungary, June 1979.
- [3]. J. Miller, 1st International Workshop on Space Radiation Research and 11th Annual NASA Space Radiation Health Investigators, Workshop Arona (Italy), May 27–31, 2000, Physica Medica–Vol. XVII, Supplement 1, 2001.
- [4]. I. Schall, D. Schardt, H. Geissel, H. Irnich, E. Kankleit, G. Kraft, A. Magel, M. Mohar, G. Mützenber, F. Nickel, C. Scheidenberger, W. Schwab, Nucl. Instr. and Meth. B 117, 221 (1996).
- [5]. I. Schall, D. Schardt, H. Geissel, H. Irnich, E. Kankleit, G. Kraft, A. Magel, M. Mohar, G. Mützenber, F. Nickel, C. Scheidenberger, W. Schwab, L. Sihver; Adv. Space Res. B 17, 87 (1996).
- [6]. C. Von Essen, M. Bagshaw, S. Bush, A. Smith, M. Kligerman, "Long-Term Results of Pion Therapy at Los Alamos" (September 1987), Int. J. Radiat. Oncol. Biol. Phys. 13, 1389 (1987).
- [7]. B. George Goodman, for TRIUMF Cancer Therapy with Pions, Proceedings of the 13th International Conference on Cyclotrons and their Applications, Vancouver BC, Canada, 6 – 10 July, 242 (1992).
- [8]. Petti and Lennox, Ann. Rev. Nuclear & Particle Science 44, 154 (1994).
- [9]. <http://www.klinikum.uni-heidelberg.de/index.php?id=113005&L=1>
- [10]. CERN COURIER Nov 23, 2011.
- [11]. J. Benecke, T. T. Chou, C. N. Yang, and E. Yen, Phys. Rev. 188, 2159 (1969).
- [12]. Fu-Hu Liu, Chinese Journal of Physics 40, 159 (2002).
- [13]. M. S. Ahmad, M. Q. R. Khan, and R. Hasan, Nucl. Phys. A 499, 821 (1989).
- [14]. W. R. Webber, Proceedings of the international Cosmic Ray Conference, Vol. 8, P. 65, Moscow, USSR (1987).
- [15]. P. L. Lindstorm, D. E. Greiner, H. H. Heckman, and B. Cork, Lawrence Berkeley Laboratory Report, LBL–3650, 1975.
- [16]. D. L. Olson, B. L. Berman, D. E. Grenier, H. H. Heckman, P. J. Lindstrom, and H. J. Crawford, Phys. Rev. C 28, 1602 (1983).
- [17]. M. S. El-Nagdy, A. Abdelsalam, Z. Abou-Moussa, and B. M. Badawy, Can. J. Phys. 91, 737 (2013).
- [18]. C. F. Powell, F. H. Fowler, and D. H. Perkins, The Study of Elementary Particles by the Photographic Method, Pergamon Press. London, New York, Paris, Los Angles, 474 (1958).
- [19]. H. Barkas, Nuclear Research Emulsion, Vol. I, Technique and Theory Academic Press Inc. (1963).
- [20]. S. Yu. Shmakov and V. V. Uzhinskii, Com. Phys. Comm., 54, 125 (1989).
- [21]. M. El-Nadi, N. Ali-Mossa, and A. Abdelsalam, IL Nuovo Cimento A 110, 1255 (1998).
- [22]. M. S. El-Nagdy, M. M. Sherif, O. Wahba and F. A. Abdel-Wahed, Mod. Phys. Lett., A 20, 18 (2005).
- [23]. A. Abdelsalam, M. S. El-Nagdy, and B. M. Badawy, Can. J. Phys. 89, 261 (2011).
- [24]. A. Abdelsalam, E. A. Shaat, Z. Abou-Moussa, B. M. Badawy, and Z. S. Mater, Radiation Physics and Chemistry 91, 1 (2013).
- [25]. K. N. Mukhin, Experimental Nuclear Physics Vol. I, Physics of Atomic Nuclei, Mir Publishers, Moscow, Russia, 1st published in English 1987.
- [26]. <http://www.srim.org/>